RSC Advances

ROYAL SOCIETY OF CHEMISTRY

www.rsc.org/advances

Graphical Abstract

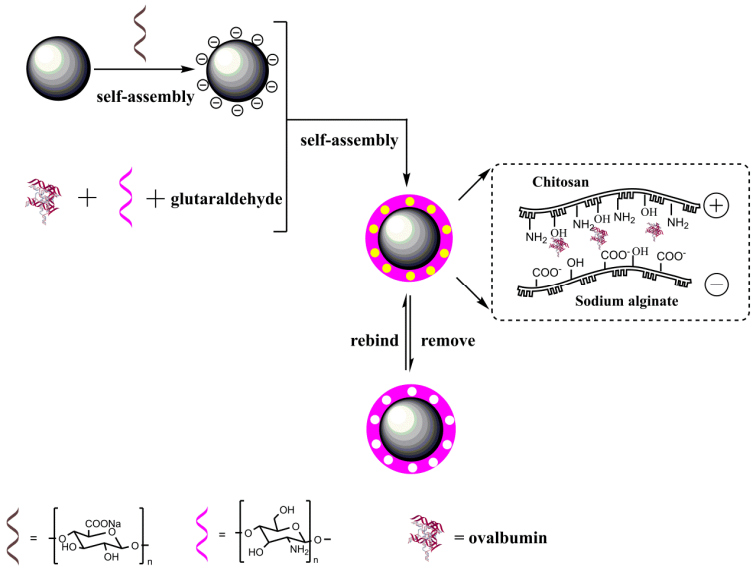

Facile and green synthesis of polysaccharide-based magnetic molecularly imprinted nanoparticles for protein recognition

Ruixia Gao[a,*], Siqi Zhao[a], Yi Hao[a,b], Lili Zhang[a,b], Xihui Cui[a,b],

Dechun Liu[c], Yuhai Tang[a,b,*]

[a] Institute of Analytical Science, School of Science, Xi'an Jiaotong University, Xi'an 710049, China.

[b] College of Pharmacy, Xi'an Jiaotong University, Xi'an 710061, China.

[c] Department of Hepatobiliary Surgery, First Hospital of Xi'an Jiaotong University Xi'an 710061, China

* Corresponding authors: Tel.: +86 29 82655399; fax: +86 29 82655399.

E-mail: ruixiagao@mail.xjtu.edu.cn (R. Gao); tyh57@mail.xjtu.edu.cn (Y. Tang).

Abstract

In this study, a facile and green approach to prepare the core-shell magnetic molecularly imprinted nanoparticles based on a layer-by-layer assembly and surface imprinting technique was developed. Two types of natural polysaccharides (sodium alginate and chitosan) were firstly employed as hydrophilic double-monomers to synthesize water-compatible imprinted nanomaterials *via* a two-step self-assembly strategy for recognizing protein ovalbumin. The obtained products exhibited a desired level of magnetic susceptibility (45.30 emu g^{-1}), resulting in the convenient and highly efficient separation process. The imprinted layer with thickness about 8 nm was homogeneously coated on the surface of Fe_3O_4, which was favorable for the fast mass transfer and rapid binding kinetics. The results of adsorption experiments showed that the saturation adsorption capacity of imprinted products could reach 92.22 mg g^{-1} within 40 min, which illustrated the high binding capacity. Meanwhile, the imprinting factor was as high as 4.07, demonstrating the potential selectivity of the prepared products. More importantly, the test of validation suggested that the proposed strategy would be a general method for imprinting different proteins in aqueous media by virtue of the peculiarity of polysaccharides as well as the efficient preparation process.

Keywords: polysaccharide; magnetic separation; surface imprinting; protein

1. Introduction

The molecular imprinting technique (MIT) has been recognized as a versatile strategy for offering a way to construct tailor-made polymers with high affinity and selectivity towards the targeted analytes.[1-2] Owing to their high selectivity, low cost, chemical stability, and easy fabrication, the molecularly imprinted polymers (MIPs) have been explored for various applications in drug delivery,[3] biosensors,[4] molecules recognition,[5] and catalysis.[6] Nowadays, although molecular imprinting has proven to be particularly successful for small molecules, recognition of water-soluble biological macromolecules, in particular proteins, using molecular imprinting is still challenging, which is primarily related to the complexity of biomolecular size, conformational flexibility, and solubility.[7,8] It is gratifying that various methodologies have been exploited to prepare the protein-imprinted polymers successfully, such as surface imprinting, epitope-mediated imprinting, metal coordination procedure, and protein imprinted hydrogel.[9-12]

Apart from the development of efficient synthesis methods for imprinting protein, selecting the optimum functional monomer with high affinity for the template protein also has profound influence on obtaining the ideal imprinted polymers. Due to inherent properties of proteins, resulting in imprinting generally only was performed in aqueous media, many conventional functional monomers applied to imprint small molecules exhibited quite difficult for protein.[13] To overcome this limitation, many researchers have focused on the development of water-compatible MIPs for imprinting protein and achieving recognition, in which some low-cost monomers

possessing hydrophilicity and multi-functional groups are employed, such as dopamine and phenylboronic acid.[14-16]

In recent years, natural polysaccharides also have attracted great attention in imprinting protein due to their abundant raw materials, great hydrophilicity, nontoxicity, and biocompatibility. Some works (listed in Table S1) of protein-imprinted polymers with polysaccharides such as cyclodextrin, chitosan, cellulose, and alginic acid have been reported.[17-20] Zhang *et al*. prepared imprinted silica beads for selective recognition of lysozyme adopting acryloyl-cyclodextrin as functional monomer.[17] Li *et al*. grafted imprinted polymer on chitosan microsphere surface by sol-gel process for protein recognition.[18] Zhang *et al*. prepared protein molecularly imprinted cellulose ester filter membranes using acrylamide as functional monomer for selective permeation of bovine serum albumin (BSA).[19] Li *et al*. synthesized protein-imprinted polyurethane-grafted calcium alginate hydrogel microspheres which showed improved mechanical stability and recognition specificity.[20] Among of these polysaccharides, chitosan (CS), a kind of alkaline polysaccharide with plentiful amino and hydroxyl functional groups which can interact with protein through multiple hydrogen bonds, has aroused the most extensive interest as an attractive candidate monomer for imprinting protein.[21-24] The magnetic-chitosan MIPs achieved more superiority owning to their fast magnetic separation and satisfactory binding capability. Guo *et al.* has synthesized the lysozyme-imprinted polymers using magnetic chitosan submicrospheres as the support materials.[25] Chen *et al.* has prepared chitosan-coated magnetic nanoparticles

modified carbon nanotubes to imprint BSA.[26] While CS enjoyed some advantages in these works, their preparation strategies were rather complicated, involving heating, multi-step graft, and modification. There is still a lot of room for exploring facile polymerized method. Interestingly, sodium alginate (SA) is another type of natural and hydrophilic polysaccharide containing carboxylic and hydroxyl groups. As with CS, the excellent biological and chemical properties of SA also have been widely documented and applied in the field of chemical biology.[27,28] More excitingly, SA, as an anionic polysaccharide, can layer-by-layer assemble with CS (a cationic polysaccharide) through the strong electrostatic interaction of the carboxylic groups of the SA and the amino groups of the CS.[29] Given the aforementioned characteristics, SA can serve as bridge for linking CS and support, which impels CS to coat on support materials easily under a mild condition.

Inspired by the above remarkable properties of two polysaccharides, we report a facile two-step method to prepare core-shell magnetic protein imprinted nanoparticles (MP-MIPs) based on the self-assembly of two oppositely charged polysaccharides. Fe_3O_4 nanoparticles were selected as the support and modified with SA. The preparation of MP-MIPs was carried out by the electrical interaction of SA and CS as well as the cross-linking of glutaraldehyde, which used ovalbumin (OVA) as the template protein. In this process, SA not only facilitated to attract CS to coat on the magnetic particles, but interacted with protein by functional groups in the chains. The resultant MP-MIPs possessed a uniform imprinted layer, was favorable for the fast mass transfer and rapid binding kinetics. The excellent molecular recognition ability

for OVA and other proteins proved that SA and CS were appropriate for imprinting proteins in a mild condition. To our knowledge, this is the first time for combination of two polysaccharides (SA and CS) to synthesize the water-compatible MIPs for applying to different proteins. Moreover, the developed method in this work subtly use the electrical properties of two polysaccharides and directly imprint protein at room temperature without multi-step modification and the assist of some organic monomers, which is more efficient as well as green and would have a great potential prospect in applications.

2. Experimental

2.1. Reagents and Materials

Ovalbumin (OVA, pI 4.7, MW 43.0 kDa, ≥96%), bovine hemoglobin (BHb, pI 6.9, MW 64.0 kDa,, ≥95%), bovine serum albumin (BSA, pI 4.9, MW 66.0 kDa, ≥ 97%) and lysozyme (Lyz, pI 11.2, MW 13.4 kDa, ≥98%) were purchased from Sigma. Sodium alginate (SA, MW 398.31, AR) was purchased from Aladdin Chemical Company. Chitosan (CS) powder was purchased from Jinke Biochemical Chemicals Ltd. (Zhejiang, China), with viscosity-average MW of about 40000 and deacetylation degree of about 90%. Ferric chloride hexahydrate ($FeCl_3 \cdot 6H_2O$, 99%, AR), anhydrous sodium acetate (NaOAc, 99%, AR), sodium chloride (NaCl, 99.5%, AR), ethylene glycol (EG, AR), glutaraldehyde (50%, AR), polyethylene glycol (PEG, AR) and ethanol (99.7%, AR) were provided by Tianjin Fuyu Chemicals Ltd. The highly purified water was obtained from a WaterPro water system (Axlwater Corporation, TY10AXLC1805-2, China) and used throughout the experiments. phosphate buffer

132 solution (pH=4.7, 10 mM) was used as the working medium. All the chemicals were
133 used as received and without further treatment.

134 **2.2. Preparation of Fe_3O_4 nanoparticles**

135 The Fe_3O_4 nanoparticles (denoted as Fe_3O_4) were prepared through a
136 solvothermal reaction. Briefly, $FeCl_3 \cdot 6H_2O$ (1.013 g), NaOAc (2.70 g) and PEG
137 (0.075 g) were dissolved in EG (15 mL) in a Teflon-lined stainless-steel autoclave,
138 sealed to heat at 200 °C and reacted for 12 h to obtained black products. The resultant
139 black products were washed with highly purified water for several times, and then
140 dried in vacuum for further use.

141 **2.3. Preparation of Fe_3O_4@SA**

142 To prepare alginate-modified magnetic nanospheres, the obtained Fe_3O_4 (50 mg)
143 was added into SA solution (1.5 $mg \cdot mL^{-1}$, in 0.1 M NaCl, 30 mL), ultrasonicated for
144 30 min and stirred vigorously at room temperature for another 12 h. The SA wrapped
145 Fe_3O_4 (Fe_3O_4@SA) were collected by a magnet and washed with ultrapure water to
146 remove the unbound reagents.

147 **2.4 . Preparation of MP-MIPs and MP-NIPs**

148 First, CS (90 mg) was dissolved into 30 mL of phosphate buffer solution. And
149 then, the Fe_3O_4@SA (50mg) and OVA (15 mg) were added to the above CS solution.
150 After incubation by stirring for 1 h, 10 μL of glutaraldehyde was added. Then, the
151 mixture was allowed to react for 6 h and the resultant nanoparticles were separated
152 using a magnet and washed repeatedly with 0.5 M NaCl to remove the template
153 protein until no adsorption was detected by UV-vis spectrophotometer at about 280

nm. Finally, the as-prepared imprinted nanoparticles were dried under vacuum for further use. The non-imprinted magnetic nanomaterials (denoted as MP-NIPs) were prepared adopting the same procedures in the absence of template.

2.5. Characterization

The morphology and structure of the Fe_3O_4 and MP-MIPs were examined using JSM-7000F scanning electron microscope and JEM-2100 transmission electron microscope (JEOL Co., Japan). The identifications of the crystalline phase of Fe_3O_4 and MP-MIPs were investigated by a Rigaku D/max/2500v/pc (Japan) X-ray diffractometer with a Cu Kα source. The 2θ angles probed were from 20° to 80° at a rate of 4° min^{-1}. Magnetic properties were measured using a vibrating sample magnetometer (VSM) (LDJ 9600-1, USA). Zeta potentials were measured by a Zeta Potential Analyzer (Zetasizer Nano S90, Malvern).

2.6. Binding experiments of MP-MIPs and MP-NIPs

To evaluate the recognition properties of MP-MIPs and MP-NIPs, we performed a series of adsorption experiments including the adsorption isotherms, adsorption kinetics, and the selectivity of MP-MIPs. In all the experiments, the mass of MP-MIPs or MP-NIPs was 10 mg and the volume of the protein solution was 5 mL in a phosphate buffered solution (pH 7.0, 10 mM). The concentration of OVA in the supernatant was measured by UV-vis spectrophotometer. The adsorption capacity (Q, mg g^{-1}) of protein bound to MP-MIPs or MP-NIPs was calculated using equation (1).

$$Q = \frac{(C_i - C_f)V}{W} \qquad (1)$$

where C_i (mg mL^{-1}) is the initial concentration of protein solution, C_f (mg mL^{-1}) is the final concentration in the supernatant of protein solution after adsorbed by MP-MIPs or MP-NIPs, V (mL) is the volume of protein solution, and W (mg) is the weight of MP-MIPs or MP-NIPs.

The isothermal study was conducted through using different initial concentrations (0.10 to 0.90 mg mL^{-1}) of the solution of OVA and kept shaking the mixture for 40 min at room temperature. The adsorption kinetics was investigated by changing the adsorption time from 0 to 60 min while keeping the initial concentration of OVA constant at 0.50 mg mL^{-1}, and the MP-MIPs also were magnetically separated from the solution. Then, the MP-MIPs were isolated by a magnet and the residual OVA in the supernatant was determined by UV-vis spectrophotometer.

The selectivity experiments were carried out by adopting single-type-protein solutions. The MP-MIPs or MP-NIPs were added to different single-type-protein solutions (OVA, BSA, BHb, and Lyz) at a concentration of 0.50 mg mL^{-1}, respectively. The mixtures were incubated for 40 min at room temperature. Then, the separation and determination procedures were conducted as described earlier in the adsorption kinetics experiments. The imprinting factor (*IF*) and selectivity coefficient (*SC*) were used to evaluate the selectivity of MP-MIPs and MP-NIPs towards OVA and competitive proteins, which are calculated by equations (2) and (3).

$$IF = \frac{Q_{\mathrm{MIPs}}}{Q_{\mathrm{NIPs}}} \quad (2)$$

$$SC = \frac{IF_{\mathrm{TEM}}}{IF_{\mathrm{COM}}} \quad (3)$$

Where Q_{MIPs} and Q_{NIPs} (mg g^{-1}) represent the adsorption capacity of proteins for MP-MIPs and MP-NIPs. IF_{TEM} and IF_{COM} are the imprinting factors for the template and competitive protein.

2.7 Generality investigation

The generality of this approach was evaluated by using another three magnetic molecularly imprinted nanoparticles (denoted as MP-MIPs-BSA, MP-MIPs-BHb, and MP-MIPs-Lyz) generated in the same way as that of MP-MIPs (**see 2.4**) except for adopting BSA, BHb, and Lyz as the template protein, respectively. The full cross-adsorption of the four protein-imprinted nanomaterials along with the MP-NIPs was investigated by adsorbing the corresponding template protein and the three other proteins. 10 mg of MP-MIPs or MP-NIPs was incubated with 5 mL of the phosphate buffered solution (pH 7.0, 10 mM) of OVA, BSA, BHb, and Lyz at a concentration of 0.50 mg mL^{-1} at room temperature for 40 min, respectively. Then, the extraction and detection procedures were conducted as described earlier in the binding experiments.

3. Results and discussion

3.1. Preparation of the MP-MIPs

Fig. 1 describes the major two steps of preparing MP-MIPs *via* a self-assembly strategy. In this study, two kinds of natural polysaccharides were selected as functional monomers for imprinting OVA. First, Fe_3O_4 nanoparticles were initially treated with SA to obtain SA-modified nanoparticles. The surface of the Fe_3O_4@SA exposed abundant carboxylic and hydroxyl groups, which could bind amino acids

present in template proteins through hydrogen-bond interaction and further react with CS by electrostatic adsorption. After that, CS was assembled onto the surface of magnetic nanoparticles to form shells by using SA as a mediator and glutaraldehyde as the cross-linker. Meanwhile, the CS containing amino and hydroxyl functional groups played the role of a functional monomer to associate with the template protein by hydrogen-bond. And thus, under the impetus of multi-hydrogen interaction among proteins and functional groups of polysaccharides, template proteins were embedded into the crosslinked shells successfully. After washing with the 0.5 M NaCl solution, the MP-MIPs possessing the suitable imprinted shells with recognition sites complementary to OVA were obtained. The aforementioned imprinting process was carried out at room temperature, which was simple, green and feasible.

3.2. Optimization of MP-MIPs preparation conditions

Generally, the amounts of monomer in the synthesis process affect the affinity and imprinting efficiency of MIPs. Therefore, to obtain more effective MIPs, the influence of different amounts of CS was evaluated ranging from 30 mg to 150 mg. The results of the *Q* and *IF* were presented in **Fig. 2**. It was observed that the *Q* and *IF* increased along with the increasing of the mass of CS from 30 mg to 90 mg. When the amount of CS was 90 mg, MP-MIPs exhibited the best adsorption ability to OVA. However, the *Q* and *IF* decreased when the mass of CS was higher than 90 mg. The main reason may be that lower amount of CS can not accommodate adequately template proteins and induce less binding sites in MP-MIPs, but over-high ones may produce higher mass transfer resistance and non-specific binding capacity. As a result,

the amount of 90 mg was chosen for the polymerization of MP-MIPs.

In this study, SA was introduced to attract CS onto the surface of Fe_3O_4 and promote the polymerization of CS. To demonstrate the role of SA, the mass ratios of SA and CS (1:3, 1:2, 1:1) were investigated. As shown in **Table S2**, when the mass ratio of SA and CS was 1:2, MP-MIPs exhibited the best adsorption ability to OVA in *Q* and *IF*. When the mass ratio of SA and CS was 1:3, the adsorption capacity was relatively lower. It was because that grafting SA incompletely in the first step could make coating CS shells difficult, which affect the imprinting effect. On the contrary, an excess of SA (1:1) not increased the absorption efficiency, but led to unnecessary materials consumption. Hence, the mass ratio of 1:2 was selected to imprint template protein. Besides, to further prove the bridge-function of SA, a contrast experiment was carried out through directly coating CS onto Fe_3O_4 without SA modification (Fe_3O_4@CS). It was observed from **Fig. S1**, without the first step, CS could not be deposited on the surface of magnetic nanoparticles and form obvious shells successfully. Thus, modifying Fe_3O_4 with SA is a necessary and significant step to fabricate the MP-MIPs.

3.3. Characterization of MP-MIPs

TEM and SEM were used to observe the morphological features of Fe_3O_4 and MP-MIPs. As observed in **Fig. 3 and Fig. S2**, the Fe_3O_4 and MP-MIPs exhibit a spherical structure with a relatively narrow particle size distribution. Through size analysis of the nanoparticles by the soft of Nano Measurer 1.2.5, the average diameter of Fe_3O_4 (**Fig. S2A**) and MP-MIPs (**Fig. S2B**) are 210 nm and 225 nm, corresponding

to about 8 nm thickness of imprinted layer (**Fig. 3B**) coated on the surface of Fe_3O_4. The thin imprinted shells would be beneficial to the mass transport between solution and the surface of MP-MIPs.

The zeta potentials measurements further demonstrated the process of coating polysaccharides onto Fe_3O_4 nanomaterials. As shown in **Table 1**. The surface potential of the Fe_3O_4 was 17.5 ± 0.70 mV because of the ionization of surface -OH groups. After being functionalized by negatively charged SA, the potential of Fe_3O_4@SA decreased to -35.7 ± 1.04 mV, suggesting that the intermediate negatively-charged SA could play an important role to increase the electro-adsorption of positively charged CS. Through the polymerization of CS, the potential of obtained MP-MIPs obviously increased to 3.26 ± 0.81 mV compared with that of Fe_3O_4@SA, which confirmed the layer-by-layer selfassembly of SA and CS on Fe_3O_4 surface.

The XRD patterns of the as-synthesized Fe_3O_4 and MP-MIPs were shown in **Fig. 4**. Six characteristic peaks of Fe_3O_4 (2θ=30.38°, 35.58°, 43.14°, 53.48°, 57.08°, and 62.66°) were observed for two samples in the 2θ range of 15°-80°. The peak positions at the corresponding 2θ values were indexed as (220), (311), (400), (422), (511), and (440), respectively, which matched well with the database of magnetite in the JCPDS-International Center for Diffraction Data (JCPDS Card: 19-629) file. The results demonstrated that the obtained nanoparticles were highly crystalline materials, and the crystalline of the magnetite remained unchanged during the preparation of MP-MIPs. In addition, a small peak at 2θ =20° (**Fig. 4b**) indicated the presence of amorphous CS.[30]

Magnetic property was crucial to MP-MIPs for their applications in fast separation. **Figure. 5** shows the hysteresis loops of the prepared magnetic nanoparticles. The saturation magnetization value of MP-MIPs was 45.30 emu g^{-1}, which reduced about 10 emu g^{-1} in comparison with that of the pure Fe_3O_4 (56.02 emu g^{-1}). The decrease was expected for the shielding effect of imprinted layers, however, the still high saturation magnetization value of MP-MIPs enough made them to be separated from adsorption solution easily and rapidly under an external magnet. Beside that, there were no hysteresis in all samples, and both remanence and coercivity were all close to zero, suggesting that the prepared nanoparticles were superparamagnetic.

3.4. Adsorption kinetics of MP-MIPs

The adsorption kinetics of OVA onto MP-MIPs and MP-NIPs were examined. As presented in **Fig. 6A**, the Q of the imprinted nanoparticles towards OVA had a fast trend within 30 min. As the binding period prolonged, the binding amount slowly increased, and then reached equilibrium after 40 min. In this work, due to the hydrophilicity and thin imprinted shells, template protein could approach the recognition cavities of MP-MIPs more easily and take short time to reach adsorption equilibrium. We also found that the Q of MP-MIPs to OVA kept higher as the adsorption time prolonged compared with that of MP-NIPs on account of abundant recognition cavities of the former for protein.

3.5. Adsorption isotherms of MP-MIPs

Adsorption isotherms of OVA on MP-MIPs and MP-NIPs were depicted in **Fig. 6B**. It could be noted that the amount of OVA bound to the MP-MIPs increased along

with increasing the initial concentration of the OVA solution and came to equilibrium over 0.50 mg mL^{-1}. Obviously, MP-MIPs exhibited much higher maximum binding capacity (92.22 mg g^{-1}) to OVA than that of the MP-NIPs (22.61 mg g^{-1}). The results indicated that the recognition sites of MP-MIPs had better chemical and steric matching with the template proteins.

The Langmuir and Freundlich models were applied to analyze the adsorption data. The equations can be expressed as follows:

$$\frac{C_e}{Q} = \frac{C_e}{Q_{max}} + \frac{1}{Q_{max} K_L} \quad (4)$$

$$\log Q = m \log C_e + \log K_F \quad (5)$$

where Q (mg g^{-1}) is the amount of OVA bound to MP-MIPs or MP-NIPs at equilibrium. Q_{max} (mg g^{-1}) is the apparent maximum adsorption capacity. C_e (mg mL^{-1}) is the equilibrium concentration of proteins. K_L (mL mg^{-1}) is the Langmuir constant, K_F (mg mL^{-1}) and m are the Freundlich constants which represent the adsorption capacity and heterogeneity of the system, respectively.

Through comparison of the liner correlation coefficients of two isothermal models (**Table S3**), we found that the Langmuir isotherm model (R^2>0.99) was more suitable for describing the adsorption process of OVA onto MP-MIPs and MP-NIPs than the Freundlich model (R^2<0.92). It indicated that the adsorption process of MP-MIPs and MP-NIPs towards template proteins pertained to the monolayer absorption and took place at specific homogeneous sites. Moreover, the apparent maximum adsorption capacities of OVA were 100.0 mg g^{-1} for MP-MIPs and 26.53 mg g^{-1} for MP-NIPs, which were close to the maximum adsorption capacities obtained from experiment. In

addition, the adsorption capacity of OVA in this work was higher compared with some other works.[24,31] We speculated the reason may be that the presence of CS and SA imparted the resulted imprinted nanoparticles with appropriate hydrophilicity, leading to the excellent recognition ability.

3.6. Rebinding selectivity for target protein

To investigate the selectivity of MP-MIPs nanoparticles for OVA, we dispersed MP-MIPs and MP-NIPs nanoparticles in each solution of OVA, BSA, BHb, and Lyz, with a feed concentration of 0.50 mg mL^{-1}, respectively. The pI and Mw of three control proteins employed are BHb (Mw 64.5 K, pI 6.9), BSA (Mw 66.0 K, pI 4.9), and Lyz (Mw 13.4 K, pI 11.2). As expected, the MP-MIPs exhibited a much higher binding amount for template protein OVA (99.22 mg g^{-1}) than other controls (**Fig. 7**) and the *IF* of these three proteins were much smaller than that of OVA (**Table 2**), which manifested the significant adsorption selectivity of MP-MIPs toward OVA. Nevertheless, for the MP-NIPs without specific recognition cavities, the binding amounts of four proteins also exhibited different. We suspected that this phenomenon was related to the electrostatic interaction. For protein Lyz possessing a higher pI (11.2), the *Q* of MP-NIPs was relatively lower (9.124 mg g^{-1}) due to the electrostatic repulsion between positively charged Lyz and the surface of MP-NIPs in the phosphate buffer solution (pH=7.0). Meanwhile, pI of BSA was close to OVA, their electronegativity also was close. Therefore, the rebinding of MP-NIPs to BSA was close to that of OVA and slightly higher than that of BHb. But the high adsorption capacity of MP-MIPs to template OVA compared to BSA was observed, also

suggesting that specific recognition cavities complementary in shape and size to template protein were formed in the imprinted layers. These results further proved the excellent imprinting efficiency of the present method.

3.7. Reusability of MP-MIPs

Desorption and regeneration is one of the most important properties for the application of the MIPs. To assess the reusability of the MP-MIPs, we carried out the successive adsorption-desorption process for six times using the same adsorbent. As shown in **Fig. 8**, the adsorption capacities of MP-MIPs still maintained at steady values of 91.3% for OVA after six cycles, whereas the binding amount of MP-NIPs remained almost unchanged. The decreased adsorption capacities of MP-MIPs might be ascribed to the fact that some recognition sites in the network of imprinted nanoparticles were jammed after regeneration or destructed after rewashing. Nevertheless, the adsorption affinity of MP-NIPs was nonspecific and the effect of washing steps could be negligible. These results showed the prepared MP-MIPs could be economically and effectively used for practical application.

3.8.Method validation for imprinting protein

To demonstrate the generality of the proposed imprinting method, the full cross-selectivity test was investigated using four proteins (OVA, BSA, BHb, Lyz) with a range of pI and MW as the template, respectively. The results of adsorption test to four protein-imprinted nanomaterials (MP-MIPs-OVA, MP-MIPs-BSA, MP-MIPs-BHb, MP-MIPs-Lyz) and non-imprinted nanomaterials (MP-NIPs-OVA, MP-NIPs-BSA, MP-NIPs-BHb, MP-NIPs-Lyz) were depicted in **Fig. 9**. Obviously,

for each kind of MP-MIPs based on different protein as template, the adsorption capacity of imprinted nanoparticles to template protein all exhibited a higher level than that of other proteins. Moreover, for each kind of proteins, the experimental maximum adsorption capacity of imprinted nanomaterials was higher than that of non-imprinted nanoparticles, proving that this imprinting process was valid to different kinds of proteins. Furthermore, compared with some other works for imprinting proteins, the binding amount in this work was generally satisfactory.[24, 32-34] The method validation further certified that these two kinds of polysaccharide capable of multifunctional groups and hydrophilicity were appropriate for imprinting protein.

4. Conclusion

In this study, we presented a facile two-step process for fabrication of magnetic protein imprinted nanoparticles based on layer-by-layer assembly of polysaccharides for the recognition of protein. CS and SA were employed simultaneously for imprinting template OVA, because of their considerable natural properties and abundant functional groups. Adsorption experiments demonstrated that the obtained imprinted nanomaterials exhibited comparable high capacity, fast kinetics and great selectivity. Additionally, it could be effectively recycled and reused in the presence of a magnetic field. The favorable versatility for imprinting different proteins further indicated this novel and green strategy would have great potential for the protein molecular imprinting technology.

Acknowledgements

The authors are grateful for financial support from the National Natural Science Foundation of China (Nos. 21305107), the Fundamental Research Funds for the Central Universities (Nos. xjj2013041, 08142034), China Postdoctoral Science Foundation (No. 2014M562388), and Research Innovation Program of Shanghai Municipal Education Commission (No. 14YZ138).

References

1. X. Zhou, A. Q. Wang, C. F. Yu, S. S. Wu and J. Shen, *ACS Appl. Mater. Inter.*, 2015, **7**, 11741.
2. L. K. Liu, Y. Cao, P. F. Ma, C. X. Qiu, W. Z. Xu, H. Liu and W. H. Huang, *RSC Adv.*, 2014, **4**, 605.
3. O. I. Parisi, C. Morelli, F. Puoci, C. Saturnino, A. Caruso, D. Sisci, G. E. Trombino, N. Picci and M. S. Sinicropi, *J. Mater. Chem. B*, 2014, **2**, 6619.
4. G. Sener, E. Ozgur, A. Y. Rad, L. Uzun, R. Say and A. Denizli, *Analyst*, 2013, **138**, 6422.
5. L. W. Qian, X. L. Hu, P. Guan, D. Wang, J. Li, C. B. Du, R. Y. Song, C. L. Wang and W. Q. Song, *Anal. Chim. Acta*, 2015, **884**, 97.
6. Y. Guo and T. Y. Guo, *Chem. Commun.*, 2013, **49**, 1073.
7. R. Schirhagl, *Anal. Chem.*, 2014, **86**, 250.
8. K. G. Yang, L. H. Zhang, Z. Liang and Y. K. Zhang, *Anal. Bioanal. Chem.*, 2012, **403**, 2173.
9. Z. Zhang, J. H. Li, J. Q. Fu and L. X. Chen, *RSC Adv.*, 2014, **4**, 20677.

10. Y. Z. Wang, D. Y. Li, X. W. He, W. Y. Li and Y. K. Zhang, *Anal. Bioanal. Chem.*, 2015, **182**, 1465.
11. J. X. Liu, K. G. Yang, Q. L. Deng, Q. R. Li, L. H. Zhang, Z. Liang and Y. K. Zhang, *Chem. Commun.*, 2011, **47**, 3969.
12. B. H. Kan, B. B. Lin, K. Y. Zhao, X. X. Zhang, L. Z. Feng, J. F. Wei and Y. C. Fan, *RSC Adv.*, 2014, **4**, 55846.
13. L. X. Chen, S. F. Xu and J. H. Li, *Chem. Soc. Rev.*, 2011, **40**, 2922.
14. E. Verheyen, J. P. Schillemans, M. V. Wijk, M. A. Demeniex, W. E. Hennink and C. F. V. Nostrum, *Biomaterials*, 2011, **32**, 3008.
15. M. Zhang, X. H. Zhang, X. W. He, L. X. Chen and Y. K. Zhang, *Nanoscale*, 2012, **4**, 3141.
16. Z. A. Lin, L. X. Sun, W. Liu, Z. W. Xia, H. H. Yang, and G. N. Chen, *J. Mater. Chem. B*, 2014, **2**, 637.
17. W. Zhang, L. Qin, X. W. He, W. Y. Li and Y. K. Zhang, *J. Chromatogr. A*, 2009, **1216**, 4560.
18. F. Li, J. Li and S. S. Zhang, *Talanta*, 2008, **74**, 1247.
19. M. S. Zhang, J. R. Huang, L. P. Tang, *Acta Chim. Sinica*, 2009, **67**, 2840.
20. L. X. Li, X. G. Ying, J. Q. Liu, X. Li and W. Y. Zhang, *J. Appl. Polym. Sci.*, 2015, **132**, 42140.
21. T. Y. Guo, Y. Q. Xia, J. Wang, M. D. Song and B. H. Zhang, *Biomaterials*, 2005, **26**, 5737.
22. H. M. Duan, L.L. Li, X. J. Wang, Y. H. Wang, J. B. Li, and C. N. Luo, *RSC Adv.*, 2015, **5**, 68397.

23. A. Fatoni, A. Numnuam, P. Kanatharana, W. Limbut and P. Thavarungkul, *Analyst*, 2014, **139**, 6160.

24. R. Dan, Y. Z. Wang, L. Du, S. H. Du, M. D. Huang, S. Yang and M. Zhang, *Analyst*, 2013, **138**, 3433.

25. H. Guo, D. Y. Yuan and G. Q. Fu, *J. Colloid Interf. Sci.*, 2015, **440**, 53.

26. H. J. Chen, Z. H. Zhang, L. J. Luo and S. Z. Yao, *Sensor. Actuat. B- Chem.*, 2012, **163**, 76.

27. W. Wang, X. J. Huang, J. D. Cao, P. Lan and W. Wu, *Acta Biomater.*, 2014, **10**, 234.

28. J. H. Chen, G. P. Li, Q. L. Liu, J. C. Ni, W. B. Wu and J. M. Lin, *Chem. Eng. J.*, 2010, **165**, 465.

29. L. J. Meng, W. J. Xia, L. Liu, L. Y. Niu and Q. H. Lu, *ACS Appl. Mater. Inter.*, 2014, **6**, 4989.

30. W. Jiang, W. F. Wang, B. C. Pan, Q. X. Zhang, W. M. Zhang and L. Lv, *ACS Appl. Mater. Inter.*, 2014, **6**, 3421.

31. W. X. Su, J. Rick and T. C. Chou, *Microchem. J.*, 2009, **92**, 123.

32. K. Y. Zhao, B. B. Lin, W. K. Cui, L. Z. Feng, T. Chen and J. F. Wei, *Talanta*, 2014, **121**, 256.

33. X. P. Jia, M. L. Xu, Y. Z. Wang, D. Ran, S. Yang and M. Zhang, *Analyst*, 2013, **138**, 651.

34. L. W. Qian, X. L. Hu, P. Guan, B. Gao, D. Wang, C. L. Wang, J. Li, C. B. Du and W. Q. Song, *Anal. Bioanal. Chem.*, 2014, **406**, 7221.

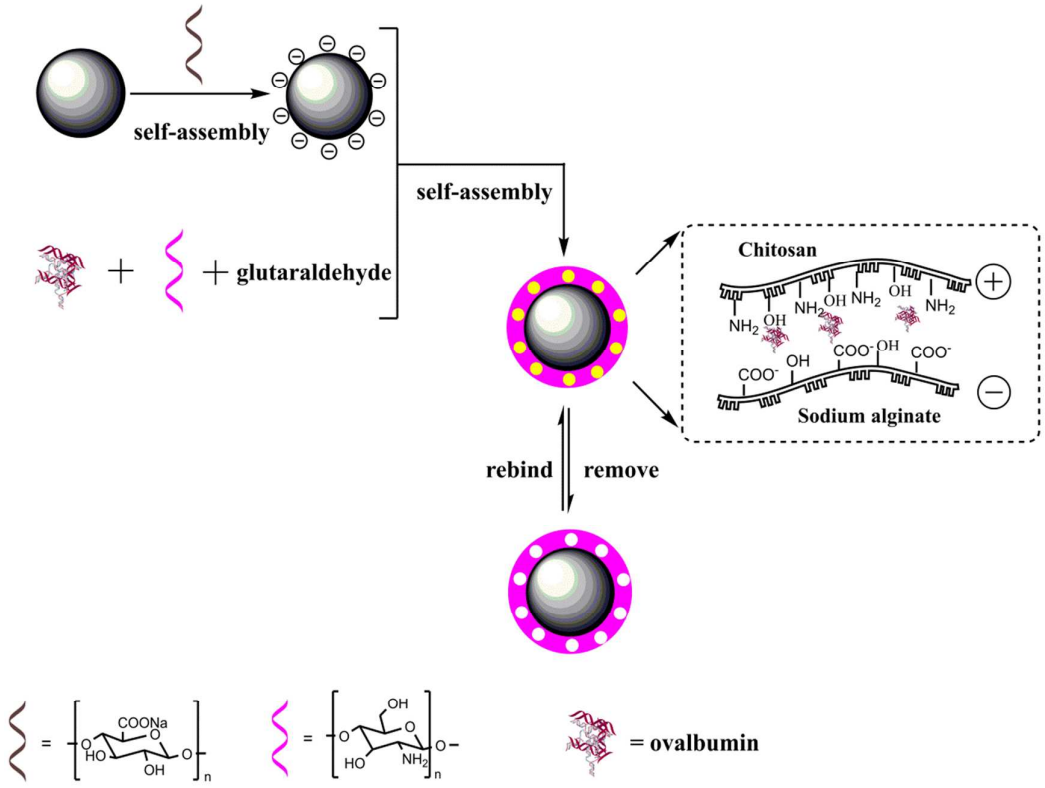

Fig. 1 Synthetic route for MP-MIPs *via* two-step process.

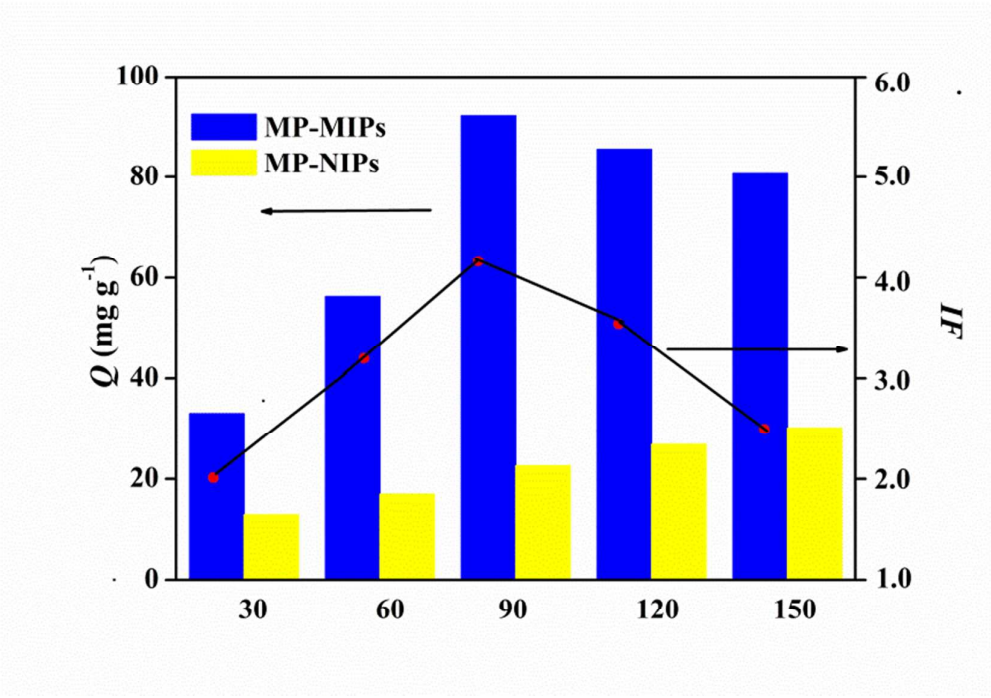

Fig. 2 Effect of the amount of CS on the imprinting performance of MP-MIPs and MP-NIPs.

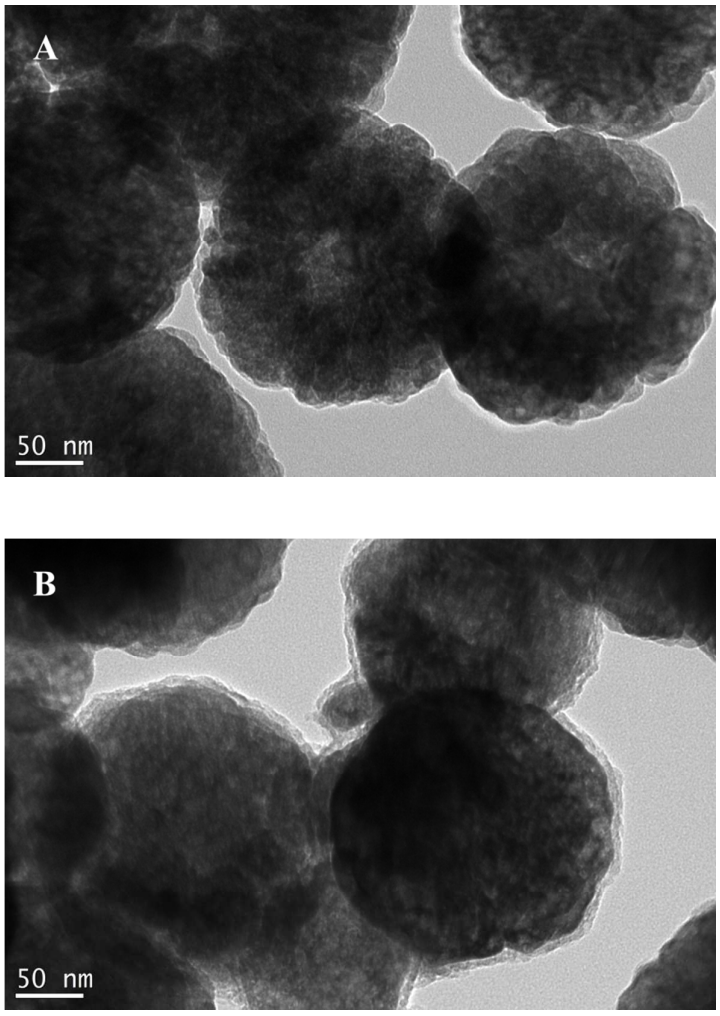

Fig. 3 TEM images of Fe_3O_4 (A) and MP-MIPs (B).

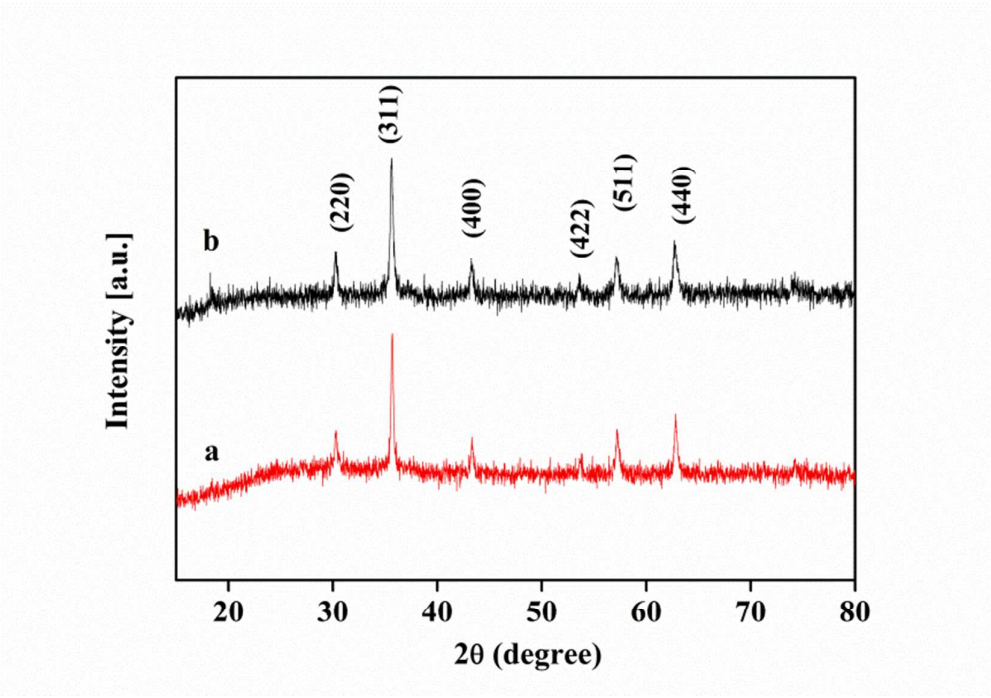

Fig. 4 XRD patterns of Fe_3O_4 (a) and MP-MIPs (b).

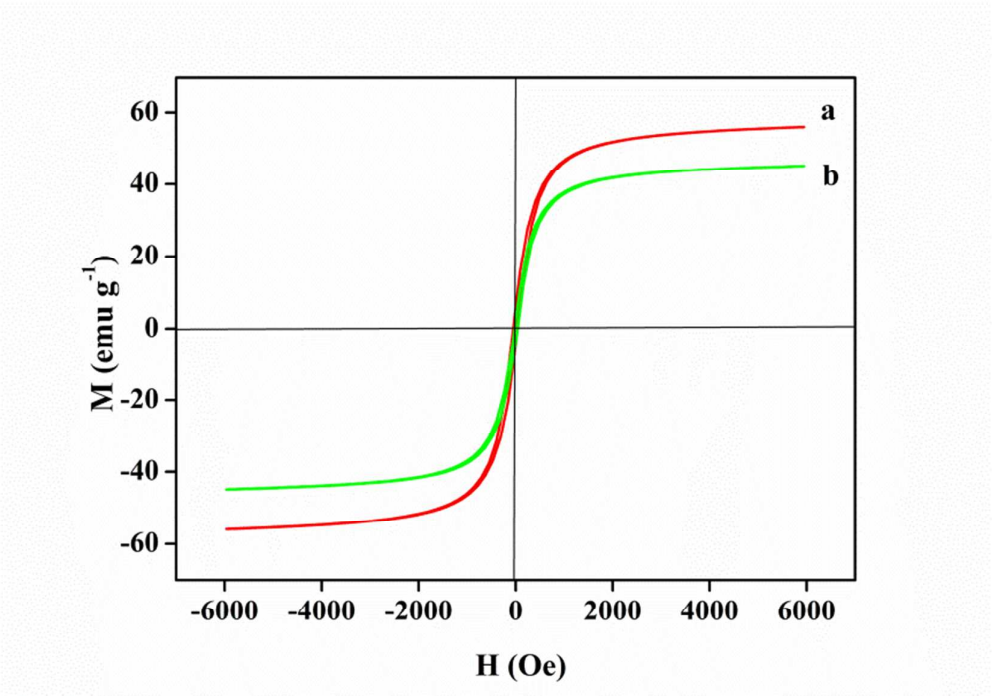

Fig. 5 The magnetization curves of Fe_3O_4 (a) and MP-MIPs (b).

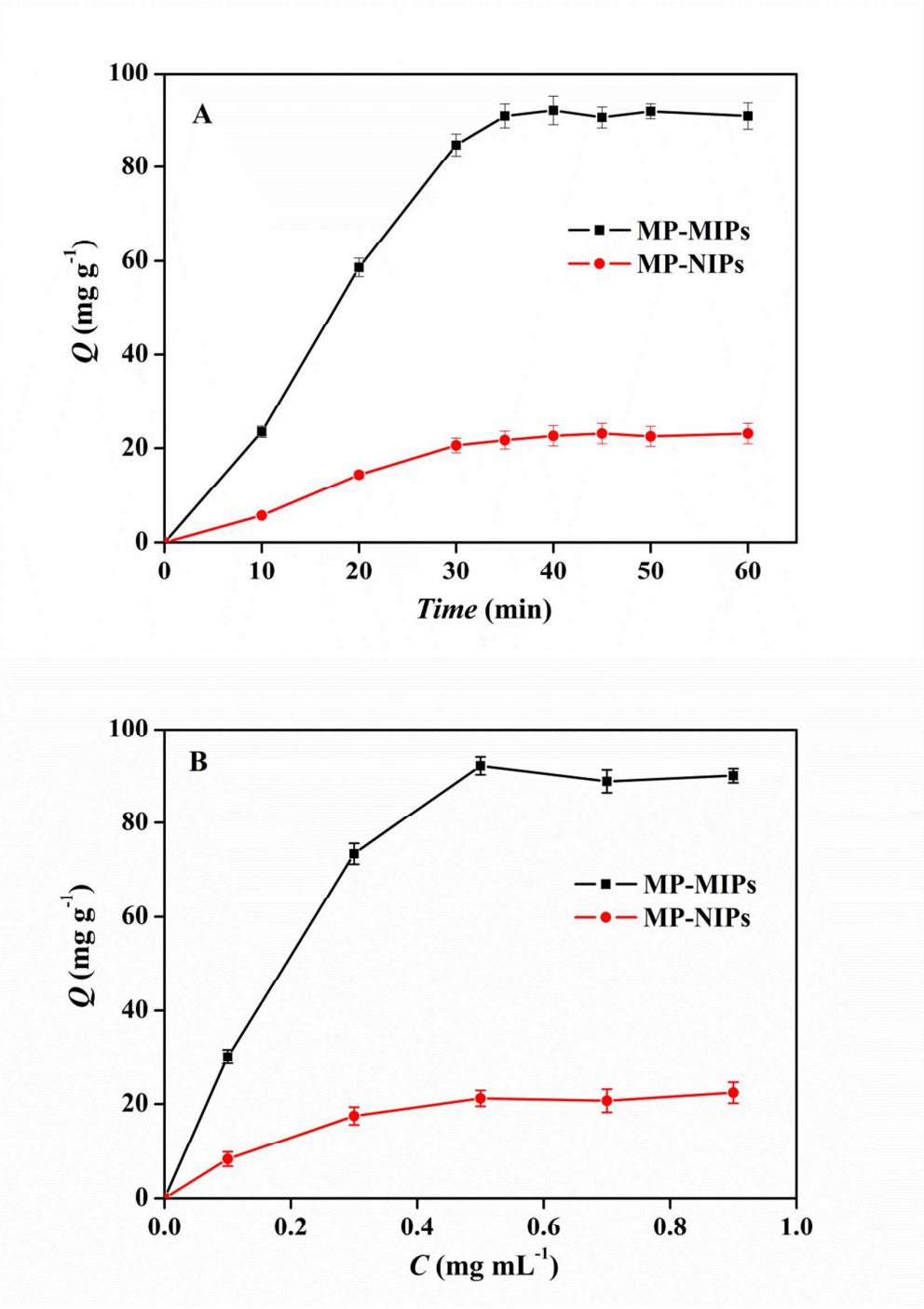

Fig. 6 Adsorption kinetics (A) and isotherms (B) of MP-MIPs and MP-NIPs towards OVA, respectively.

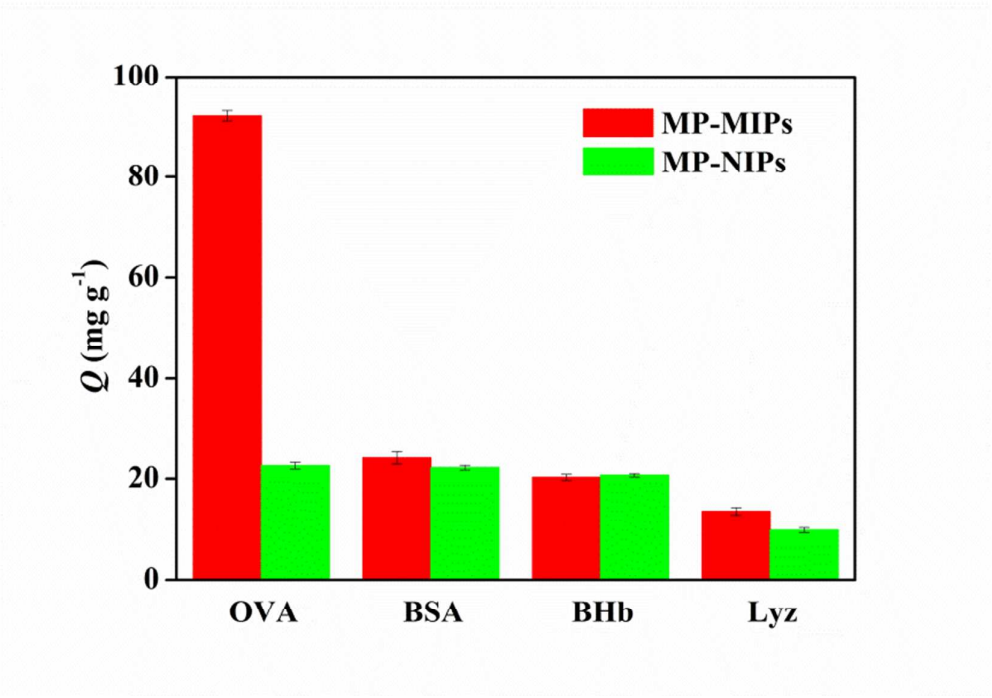

532

533 **Fig. 7** The specific adsorption capability of MP-MIPs and MP-NIPs.

534

535

536

537

538

539

540

541

542

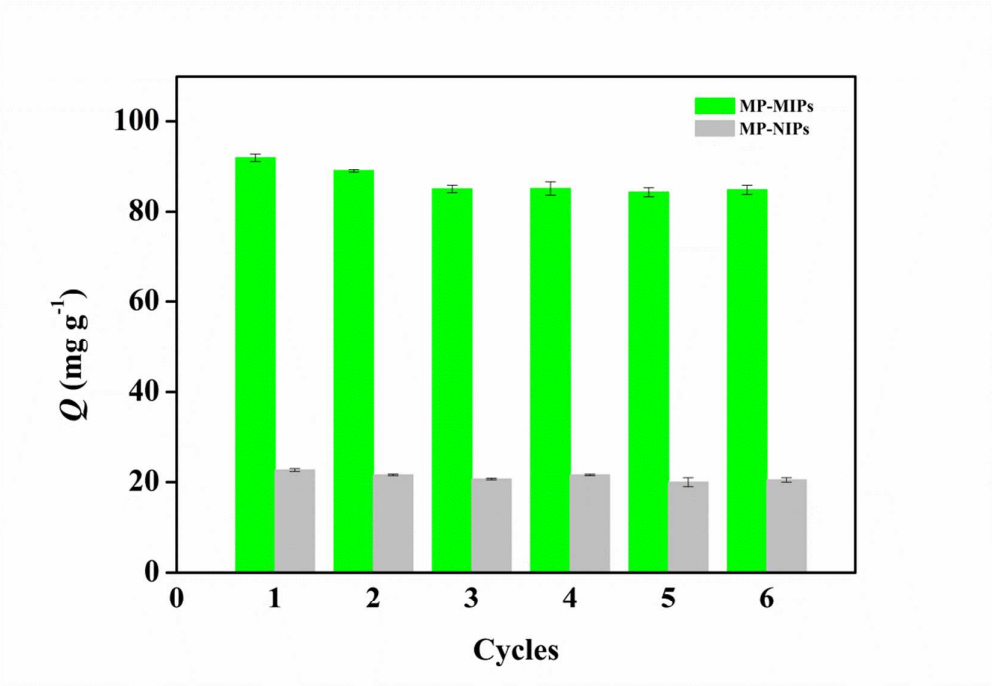

Fig. 8 The reusability of the MP-MIPs and MP-NIPs.

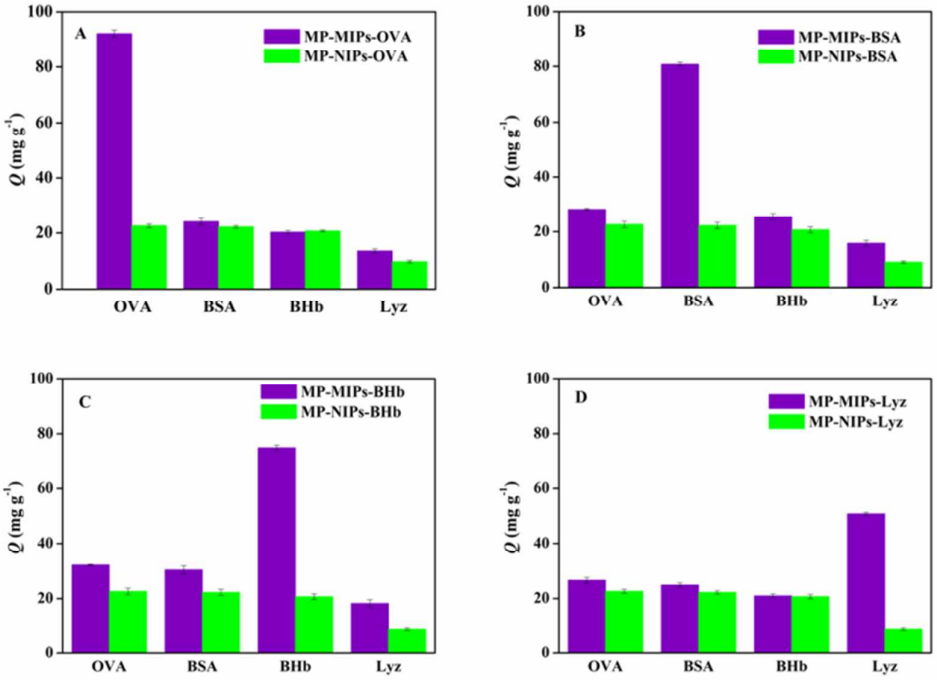

Fig. 9 Cross-selectivity of OVA, BSA, BHb, and Lyz adsorbed by MP-MIPs-OVA (A), MP-MIPs-BSA (B), MP-MIPs-BHb (C), MP-MIPs-Lyz (D) and MP-NIPs

Table 1. Zeta-potentials of the modified magnetic nanoparticles

Samples	Zeta-potentials (mV) [a]
Fe_3O_4	17.5 ± 0.70
Fe_3O_4@SA	-35.7 ± 1.04
MP-MIPs	3.26 ± 0.81

[a] Values are averaged from three measurements.

Table 2. The adsorption capacities, imprinting factors and selectivity coefficients of MP-MIPs and MP-NIPs towards template proteins and competitive proteins.[a]

Protein	Q_{MIP} (mg g^{-1})	Q_{NIP} (mg g^{-1})	*IF*	*SC*
OVA	92.22	22.61	4.07	-
BSA	24.25	22.23	1.09	3.73
BHb	20.97	20.71	1.01	4.03
Lyz	13.08	9.124	1.43	2.85

[a] In this experiment, 10 mg of MP-MIPs or MP-NIPs were incubated in the solution of OVA, BSA, BHb and Lyz with a concentration of 0.50 mg mL^{-1} for 40 min, respectively.